Pergamon

0960-0760(95)00033-X

J. Steroid Biochem. Molec. Biol. Vol. 53, No. 1–6, pp. 191–197, 1995

0960-0760/95 $9.50 + 0.00

A Molecular Model for the Interaction Between Vorozole and Other Non-steroidal Inhibitors and Human Cytochrome *P*450 19 (*P*450 Aromatase)

Luc M. H. Koymans,[1] Henri Moereels[1] and Hugo Vanden Bossche[2]*

Departments of [1]Theoretical Medicinal Chemistry and [2]Comparative Biochemistry, Janssen Research Foundation, B-2340 Beerse, Belgium

In a previous study (Vanden Bossche *et al.*, *Breast Cancer Res. Treat.* 30 (1994) 43) the interaction between (+)-*S*-vorozole and the I-helix of cytochrome *P*450 19 (*P*450 aromatase) has been reported. In the present study we extended the "I-helix model" by incorporating the C-terminus of *P*450 aromatase. The crystal structures of *P*450 101 (*P*450 cam), 102 (*P*450 BM-3) and 108 (*P*450 terp) reveal that the C-terminus is structurally conserved and forms part of their respective substrate binding pocket. Furthermore, the present study is extended to the interaction between *P*450 aromatase and its natural substrate androstenedione and the non-steroidal inhibitors (−)-*R*-vorozole, (−)-*S*-fadrozole, *R*-liarozole and (−)-*R*-aminoglutethimide. It is found that (+)-*S*-vorozole, (−)-*S*-fadrozole and *R*-liarozole bind in a comparable way to *P*450 aromatase and interact with both the I-helix (Glu^{302} and Asp^{309}) and C-terminus (Ser^{478} and His^{480}). The weak activity of (−)-*R*-aminoglutethimide might be attributed to a lack of interaction with the C-terminus.

J. Steroid Biochem. Molec. Biol., Vol. 53, No. 1–6, pp. 191–197, 1995

INTRODUCTION

According to the present nomenclature system [1] the cytochrome *P*450 isoenzyme we have studied is referred to as cytochrome *P*450 19. However, since the discovery and cloning of this *P*450 [2–4] it is known as cytochrome *P*450 aromatase and catalyzes the aromatization of androgens into estrogens. This cytochrome *P*450 enzyme system is special because the aromatization reaction involves three sequential dioxygen- and NADPH-dependent oxygenations of the substrate [2] all occurring at one single active site [5]. The androgen is first oxidized to the C-19 hydroxyandrogen and then oxidized to the 19,19-*gem*-diol, or its hydrated form, the C-19 aldehyde [6]. The mechanism of the third oxidation is still unclear. The most satisfactory mechanism involves a peroxidative attack on the C-19 methyl group. To facilitate this process a nucleophilic active site residue of *P*450 aromatase (presumably Glu^{302} [7]) is required to remove the hydrogen at the 2β-position, whereas at the same time a proton-donating residue (possibly His^{128} [8]) is needed to protonate the carbonyl group at position 3 in the A-ring. Residues His^{128} and Glu^{302} are located in or nearby a region that corresponds to the B′-helix of *P*450 101 (*P*450 cam) and in the I-helix of *P*450 aromatase, respectively. In a previous study we have shown that several non-steroidal inhibitors of aromatase are likely to interact with the I-helix of this *P*450 [9]. The I-helix contains the oxygen binding site and is highly conserved among all known cytochrome *P*450 enzymes [10]. In the I-helix of *P*450 aromatase, the oxygen binding pocket is formed by the residues Ala^{306}–Ala^{307}–Pro^{308}. These residues introduce a slight bend in the I-helix similar to the bend formed by the residues Gly^{249}–Leu^{250}–Asp^{251}–Thr^{252} in the crystal structure of *P*450 cam [11] and the corresponding residues in the crystal structures of *P*450 102 (*P*450 BM-3; [12]) and *P*450 108 (*P*450 terp; [13]). Furthermore, Glu^{302} is in close proximity to the oxygen binding sites and was shown to constitute part of the substrate binding pocket [7, 8].

In the present study we have extended our previous

Proceedings of the IX International Congress on Hormonal Steroids, Dallas, Texas, U.S.A., 24–29 September 1994.
*Correspondence to H. Vanden Bossche.

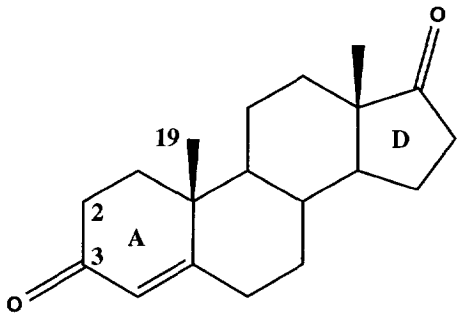

Androstenedione

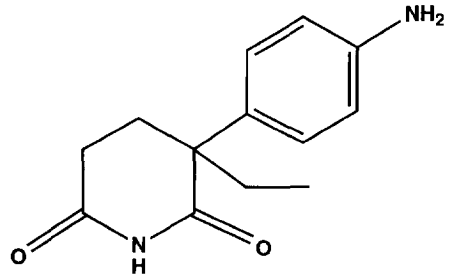

Aminoglutethimide

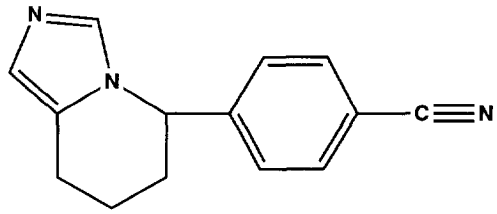

Fadrozole

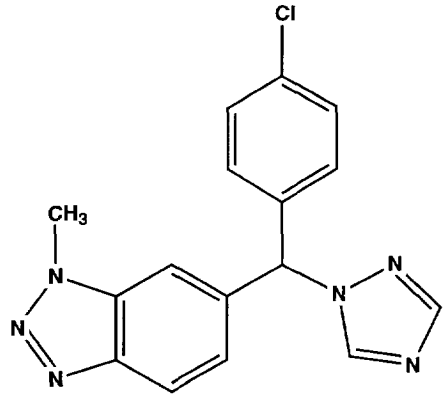

Vorozole

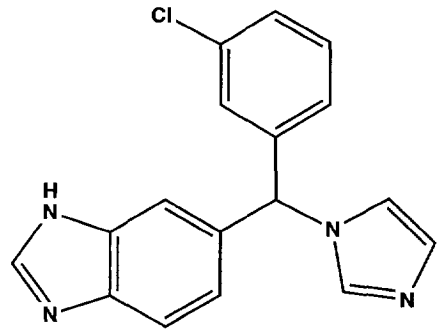

Liarozole

Fig. 1. Chemical structures of androstenedione and some non-steroidal inhibitors of *P*450 aromatase.

studies on the I-helix model of *P*450 aromatase to a model that also contains the C-terminus as part of the substrate binding pocket. In this model the interaction was studied with the natural substrate androstenedione and the inhibitors (+)-*S*-vorozole, (−)-*R*-vorozole, (−)-*S*-fadrozole, (−)-*R*-aminoglutethimide (AG) and liarozole.

METHODOLOGY

General

Five different amino acid sequences of human *P*450 aromatase have been described [4, 14–16], but these do not differ in the I-helix (residues 292–324) and C-terminal region (residues 471–486). The crystal

Fig. 2—*opposite* (A) Molecular complex of androstenedione, (B) (+)-*S*-vorozole (C) *R*-liarozole (D) (−)-*S*-fadrozole (E) (−)-*R*-vorozole, and (F) (−)-*R*-aminoglutethimide and the I-helix and C-terminus of *P*450 aromatase.

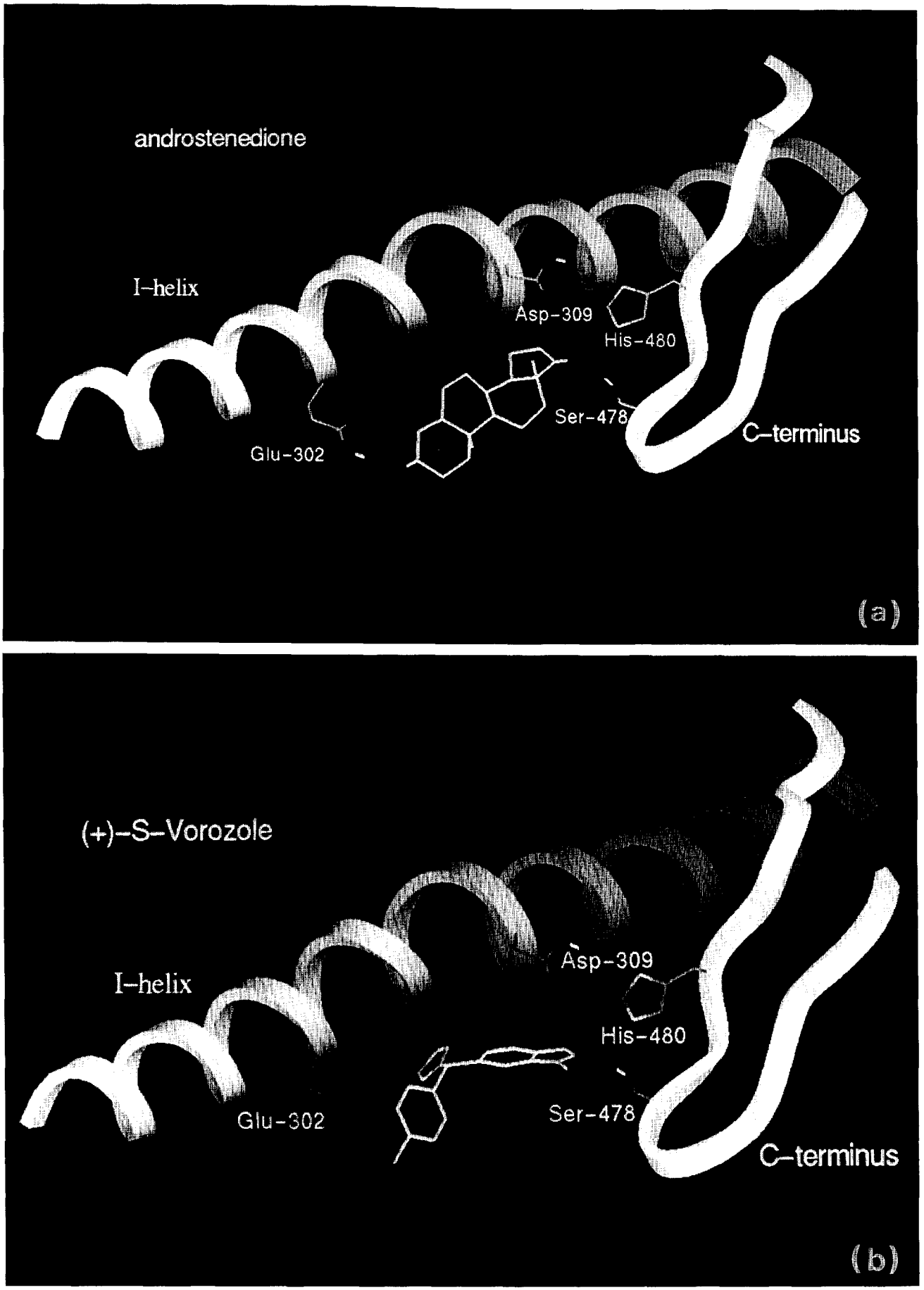

Fig. 2(a, b)—*legend opposite.*

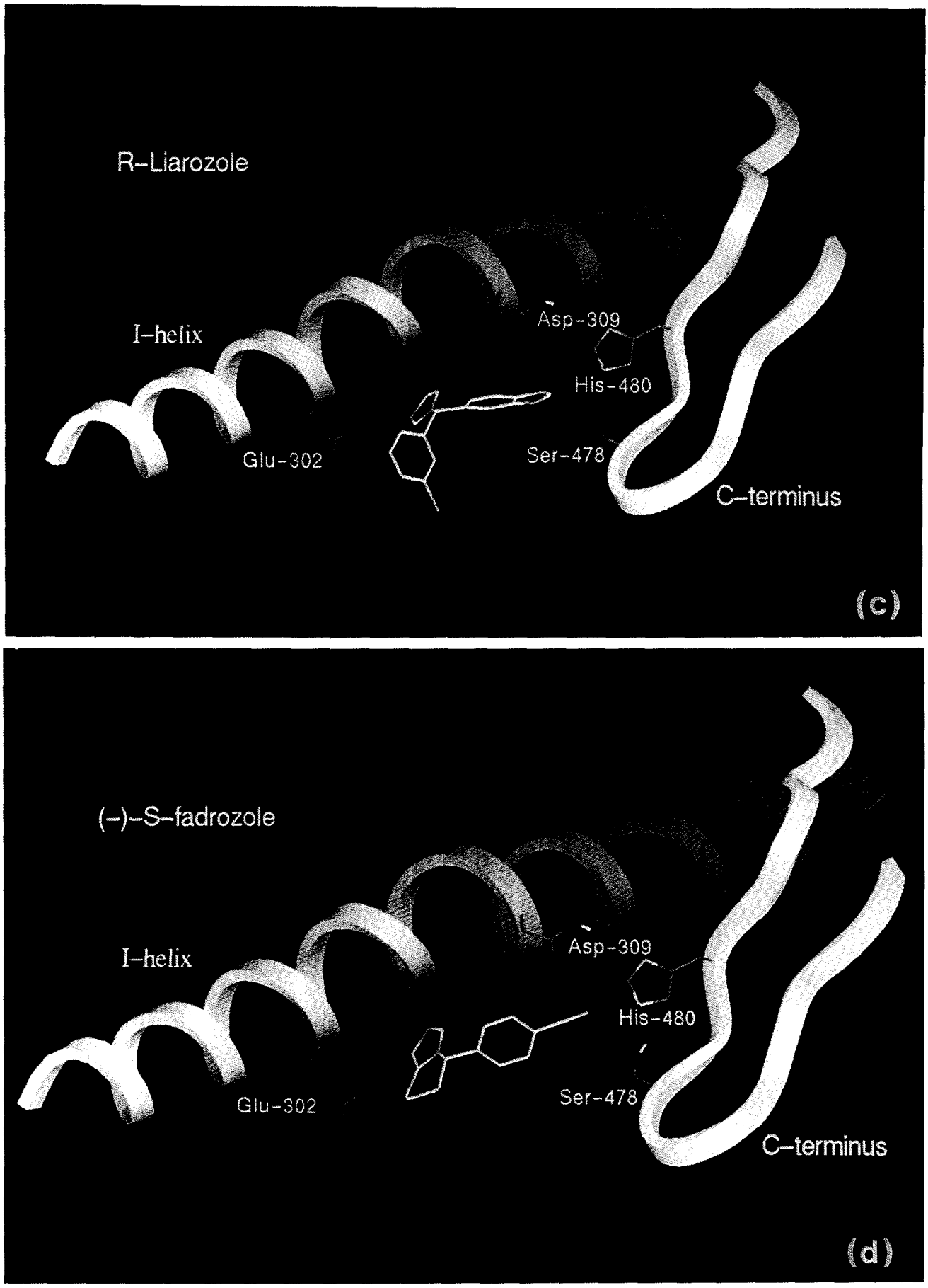

Fig. 2(c, d)—*legend on p. 192.*

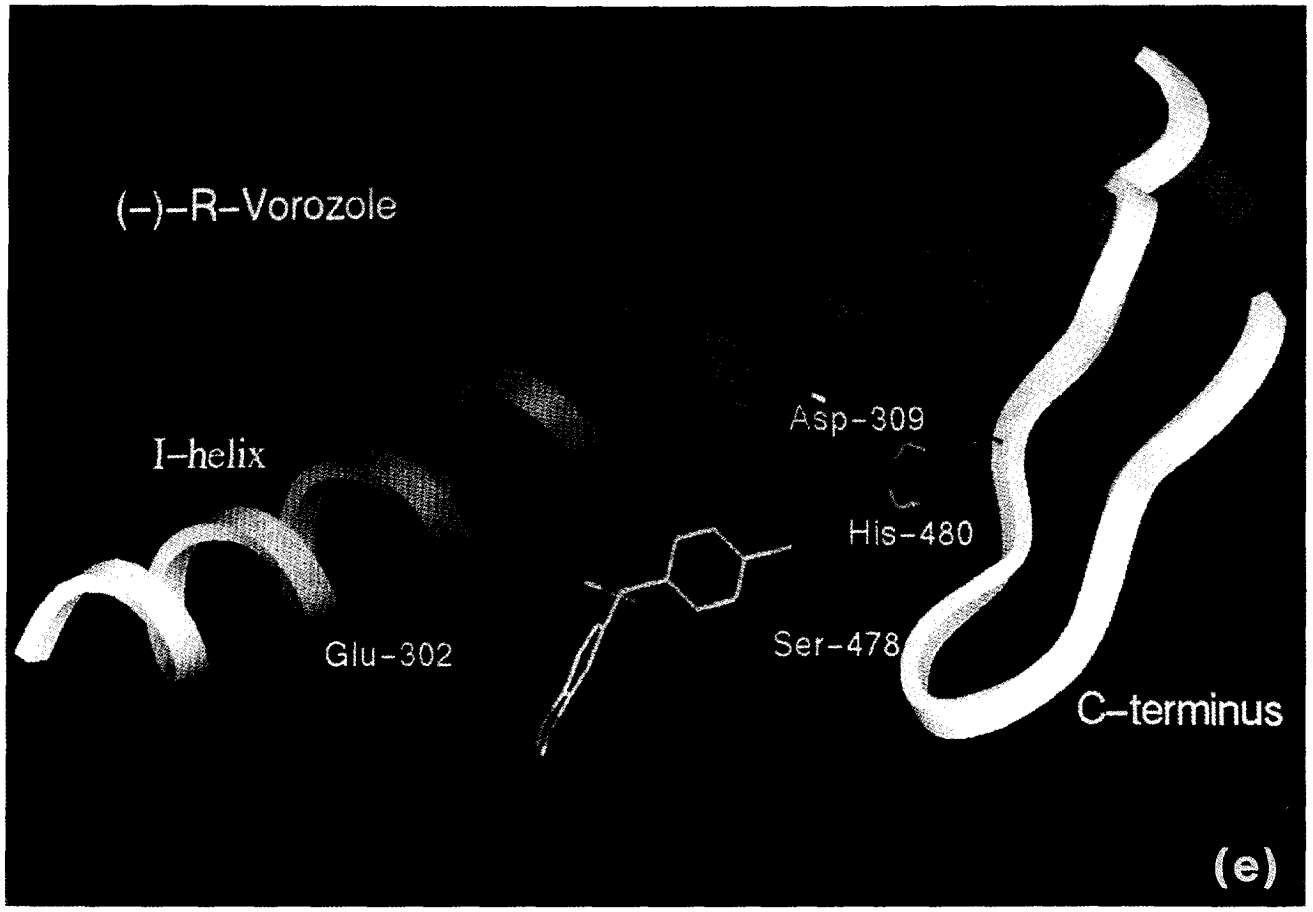

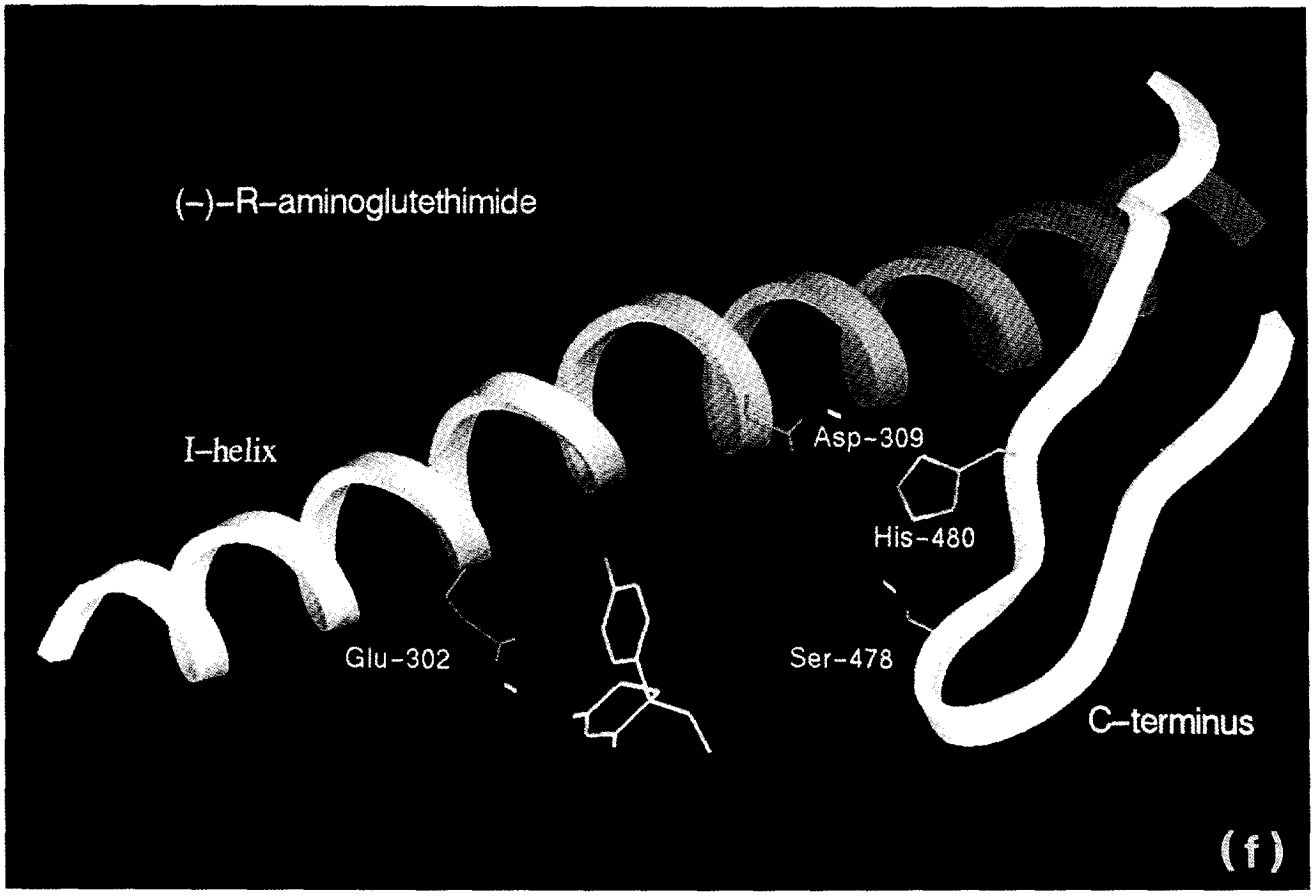

Fig. 2(e, f)—*legend on p. 192.*

structure of *P*450 cam [11] was used as a template for building the aromatase model and was taken from the Brookhaven database (pdb-code: 2CPP). All energy-minimizations were performed using BIOSYM, Insight (release 2.1.2) and Discover (release 2.8) software (BIOSYM Technologies, San Diego, CA, U.S.A.), running on a Silicon Graphics Crimson Computer equipped with stereo hardware. The starting structures were minimized by the conjugate gradient method until the rms energy derivative was less than 0.01 kcal/mol per Å. A constant dielectric $\epsilon = 1$ was used and the cut-off distance for the van der Waals and electrostatic interactions was set to a value of 8 Å. Instead of the harmonic bond stretching term, a Morse type potential form and the bond-angle cross terms option was used. During minimization the iron-ligating nitrogens of the inhibitors or the C-19 methyl group of andostrenedione were kept fixed. The backbone atoms of the I-helix and C-terminus were tethered with a penalty function of 100 kcal/Å.

Alignment of P450 cam and aromatase

The alignment of *P*450 cam and aromatase was taken from a multiple alignment containing 470 sequences describing 299 different cytochrome *P*450 genes. This alignment was made by hand using the CGEMA (Colour Graphics Editor for Multiple Alignment; [17]) software package. From this alignment it was found that residues 234–266 (I-helix) and residues 389–404 (C-terminus) of *P*450 cam correspond to residues 292–324 and 471–486 of *P*450 aromatase, respectively.

Positioning of the C-terminus relative to the I-helix

The C-terminal residues 471–486 of *P*450 aromatase were built using *P*450 cam residues 389–404 as a template. However, the position of the aromatase C-terminus had to be repositioned slightly relative to the I-helix to overcome some obvious bumps between side-chains.

Positioning of androstenedione and the inhibitors in the model

Androstenedione (Fig. 1), in its crystal structure conformation [18], was docked manually into the *P*450-model in such a way that the C-19 methyl group was in a proper position to be oxygenated (4.8 Å from the iron atom when superimposed onto the crystal structure of *P*450 cam). In concomitance, the carbonyl oxygen of the A-ring was positioned in close proximity to Glu^{302} that is suggested to play an important role in the catalysis of *P*450 aromatase and in the anchoring of substrates and inhibitors [7, 8]. In this orientation, the carbonyl oxygen of the D-ring might form a hydrogen bond with Ser^{478}, located in the C-terminus. This model was then energy-minimized keeping the C-19 methyl group of androstenedione fixed.

Subsequently, the inhibitors (−)-*R*-AG, (+)-*S*-vorozole, (−)-*R*-vorozole, *R*-liarozole and (−)-*S*-fadrozole (Fig. 1) were fitted into the *P*450-model as described earlier for vorozole [9]. The crystal structures of (+)-*S*vorozole [19], (−)-*S*-fadrozole [20] and (−)-*R*-AG [21] were used as starting conformations. Liarozole was built using the crystal structure of (+)-*S*-vorozole as a template. As the chlorine atom of liarozole is in the *meta*-position of the phenyl ring as compared to *para* for (+)-*S*-vorozole, the absolute configuration of liarozole used in this study constitutes the *R*-form. These best-fit arrangements were then energy-minimized keeping the iron-ligating nitrogen atoms fixed.

RESULTS AND DISCUSSION

Androstenedione

The energy-minimization of the aromatase model with androstenedione clearly supports the tentative model in which the orientation of androstenedione is determined by two hydrogen bonds. The A-ring carbonyl group is hydrogen bonded to Glu^{302} (I-helix), whereas the D-ring carbonyl group makes a hydrogen bond with Ser^{478} in the C-terminus [Fig. 2(a)].

The non-steroidal inhibitors

The calculations reveal that the interaction between (+)-*S*-vorozole and the *P*450 aromatase model is favoured by 3.1, 7.3 and 13.5 kcal/mol as compared to *R*-liarozole, (−)-*S*-fadrozole and (−)-*R*-AG, respectively. These binding enthalpies are in the same ranking order with the IC_{50} values of the inhibitors: ((+)-*S*-vorozole, 1.4 nM; liarozole, 4 nM; (−)-*S*-fadrozole, 5 nM; and (−)-*R*-AG, 8000 nM) [9, 22]. The difference in interaction energy between (+)-*S*- and (−)-*R*-vorozole (IC_{50} = 44.2 nM [23]) is only 4.0 kcal/mol in favour of the *S*-isomer. Ideally, this value should have been between that of (−)-*S*-fadrozole (7.3 kcal/mol) and that of (−)-*R*-AG (13.5 kcal/mol). This discrepancy might be due to the fact that (−)-*R*-vorozole adopts a conformation in the energy-minimized model that is 5.1 kcal/mol above the minimum energy conformation of (−)-*R*-vorozole. For the other inhibitors these values are: 3.5 kcal/mol for (+)-*S*-vorozole; 3.2 kcal/mol for *R*-liarozole; 1.1 kcal/mol for (−)-*S*-fadrozole and 0.2 kcal/mol for (−)-*R*-AG.

The inhibitors (+)-*S*-vorozole, *R*-liarozole and (−)-*S*-fadrozole bind to *P*450 aromatase in a similar way [Fig. 2(b–d)]. The position of the triazole and imidazole moieties relative to the iron atom is very similar to that found in the crystal structure of *P*450 cam complexed with phenylimidazoles ([24]; pdb-code: 1PHF). The 1-methyl-benztriazole ring of (+)-*S*-vorozole, the benzimidazole ring of *R*-liarozole and the cyano-substituted phenyl ring of fadrazole alll bind near Asp^{309}, Ser^{478} and His^{480}. The *R*-isomer of vorozole binds with the chlorine substituted phenyl ring in this region [Fig. 2(e)]. (−)-*R*-aminoglutethimide does not have any of these interactions

[Fig. 2(f)], which might explain its relatively large IC_{50}-value.

The chlorine-substituted phenyl ring of (+)-*S*-vorozole and *R*-liarozole, the heximidazole ring of (−)-*S*-fadrozole, the 1-methyl-benztriazole ring of (−)-*R*-vorozole and the 2,6-piperidinedione ring of (−)-*R*-AG bind in close proximity to Glu^{302} in the I-helix (Fig. 2). The described mode of binding of (−)-*S*-fadrozole is in good agreement with that found by Furet *et al.* [25]. Liarozole and (+)-*S*-vorozole are structurally very similar and have almost identical binding modes in the model of *P*450 aromatase. However, as the chlorine atom of liarozole is substituted in the *meta*-position in the phenyl ring as opposed to *para* for (+)-*S*-vorozole, the 3D-structure of (+)-*S*-vorozole fits bets with the *R*-isomer of liarozole, whereas the *S*-isomer of liarozole is very similar to (−)-*R*-vorozole.

In conclusion, molecular modeling and computation supports the model in which, in addition to the I-helix, the C-terminus of *P*450 aromatase is involved in the docking of substrates and inhibitors. This model, however, must be further validated, for example by experiments involving site-directed mutagenesis of Ser^{478} and His^{480} of *P*450 aromatase.

REFERENCES

1. Nelson D. R., Kamataki T., Waxman D. J., Guengerich F. P., Estabrook R. W., Feyereisen R., Gonzales F. J., Coon M. J., Gunsalus I. C., Gotoh O., Okuda K. and Nebert D. W.: The *P*450 superfamily: update on new sequences, gene mapping, accession numbers, early trivial names of enzymes, and nomenclature. *DNA Cell. Biol.* **12** (1993) 1–51.
2. Thompson E. A. Jr. and Siiteri P. K.: Utilization of oxygen and reduced nicotinamide adenine dinucleotide phosphate by human placental microsomes during aromatization of androstenedione. *J. Biol. Chem.* **249** (1974) 5364–5372.
3. Chen S., Shively J. E., Nakajin S., Shinoda M. and Hall P. F.: Amino terminal sequence analysis of human placenta aromatase. *Biochem. Biophys. Res. Commun.* **135** (1986) 713–719.
4. Simpson E. R., Evans C. T., Corbin C. J., Powell F. E., Ledesma D. B. and Mendelson C. R.: Sequencing of cDNA inserts encoding aromatase cytochrome *P*-450 ($P450_{AROM}$). *Molec. Cell. Endocr.* **52** (1987) 267–272.
5. Kellis J. T. Jr. and Vickery L. E.: Purification and characterization of human placental aromatase cytochrome *P*-450. *J. Biol. Chem.* **262** (1987) 4413–4419.
6. Korzekwa K. R., Trager W. F., Mancewicz J. and Osawa Y.: Studies on the mechanism of aromatase and other cytochrome *P*450 mediated deformylation reactions. *J. Steroid Biochem. Molec. Biol.* **44** (1993) 367–373.
7. Graham-Lorence S., Khalil M. W., Lorence M. C., Mendelson C. R. and Simpson E. R.: Structure–function relationships of human aromatase cytochrome *P*-450 using molecular modeling and site-directed mutagenesis. *J. Biol. Chem.* **266** (1991) 11,939–11,946.
8. Oh S. S. and Robinson C. H.: Mechanism of human placental aromatase: a new active site model. *J. Steroid Biochem. Molec. Biol.* **44** (1993) 389–397.
9. Vanden Bossche H., Moereels H. and Koymans L. M. H.: Aromatase inhibitors—mechanisms for non-steroidal inhibitors. *Breast Cancer Res. Treat.* **30** (1994) 43–55.
10. Koymans L., Donné-Op den Kelder G. M., Koppelete J. M. and Vermeulen N. P. E.: Cytochromes *P*450: their active-site structure and mechanism of oxidation. *Drug Metab. Rev.* **25** (1993) 325–387.
11. Poulos T. L., Finzel B. C. and Howard A. J.: High-resolution crystal structure of cytochrome *P*450 cam. *J. Molec. Biol.* **195** (1987) 687–700.
12. Ravichandran K. G., Boddupalli S. S., Hasemann C. A., Peterson J. A. and Deisenhofer J.: Crystal structure of hemoprotein domain of *P*450BM-3, a prototype for microsomal *P*450's. *Science* **261** (1993) 731–736.
13. Hasemann C. A., Ravichandran K. G., Peterson J. A. and Deisenhofer J.: Crystal structure and refinement of cytochrome *P*450 terp at 2.3 Å resolution. *J. Molec. Biol.* **236** (1994) 1169–1185.
14. Toda K., Terashima M., Mitsuuchi Y., Yamasaki Y., Yokoyama Y., Nojima S., Ushiro H., Maeda T., Yamamoto Y., Sagara Y. and Shizuta Y.: Alternative usage of different poly(A) addition signals for two major species of mRNA encoding human aromatase *P*-450. *FEBS Lett.* **247** (1989) 371–376.
15. Corbin C. J., Graham-Lorence S., McPhaul M., Mason J. I., Mendelson C. R. and Simpson E. R.: Isolation of a full-length cDNA insert encoding human aromatase system cytochrome *P*-450 and its expression in nonsteroidogenic cells. *Proc. Natn. Acad. Sci. U.S.A.* **85** (1988) 8948–8952.
16. Pompon D., Liu R. Y.-K., Besman M. J., Wang P-L., Shively J. E. and Chen S.: Expression of human placental aromatase in *Saccharomyces cerevisiae*. *Molec. Endocr.* **3** (1989) 1477–1487.
17. Moereels H., De Bie L. and Tollenaere J. P.: CGEMA and VGAP: A colour graphics editor for multiple alignment using a variable gap penalty. Application to the muscarinic acetylcholine receptor. *J. Comp. Aided Molec. Design* **4** (1990) 131–145.
18. Busetta B., Comberton G., Courseille C. and Hospital M.: Androst-4-en-3, 17-dione, $C_{19}H_{26}O_2$. *Cryst. Struct. Comm.* **1** (1972) 129–133.
19. Peeters O. M., Schuerman G. S., Blaton N. M. and De Ranter C. J.: Structure and absolute configuration of (+)-6-[(4-chlorophenyl)(1H-1,2,4-triazol-1-yl)methyl]-1-methyl-1H-benzotriazole (Vorozole) and its hydrobromide monohydrate. *Acta Cryst.* **C49** (1993) 1958–1961.
20. Van Roey P., Bullion K. A., Osawa Y., Browne L. J., Bowman R. M. and Braun D. G.: Structure–activity studies of non-steroidal aromatase inhibitors: the crystal and molecular structures of CGS 16949A and CGS 18320B. *J. Enzyme Inhib.* **5** (1991) 119–132.
21. Van Roey P., Bullion K. A. and Osawa Y.: Structure of (±)-aminoglutethimide. *Acta Cryst.* **C47** (1991) 829–832.
22. Vanden Bossche H.: Inhibitors of *P*450-dependent steroid biosynthesis: from research to medical treatment. *J. Steroid Biochem. Molec. Biol.* **43** (1992) 1003–1021.
23. Vanden Bossche H., Willemsens G., Roels I., Bellens D., Moereels H., Coene M-C., Le Jeune L., Lauwers W. and Janssen P. A. J.: R76713 and enantiomers: selective, nonsteroidal inhibitors of the cytochrome *P*450-dependent oestrogen synthesis. *Biochem. Pharmac.* **40** (1990) 1707–1718.
24. Poulos T. L. and Howard A. J.: Crystal structures of metyrapone- and phenylimidazole-inhibited complexes of cytochrome *P*-450cam. *Biochemistry* **26** (1987) 8165–8174.
25. Furet P., Batzl C., Bhatnagar A., Francotte D., Rihs G. and Lang M.: Aromatase inhibitors: synthesis, biological activity, and binding mode of azole-type compounds. *J. Med. Chem.* **36** (1993) 1393–1400.